Thermodynamic simulation of a hybrid thermo-solar externally fired gas turbine power plant fueled with biomass

Agustín Ghazarian, Daiana De León, Pedro Galione, Pedro Curto-Risso, Alejandro Medina, and Antonio Calvo

Citation: AIP Conference Proceedings **2033**, 040014 (2018); doi: 10.1063/1.5067050
View online: https://doi.org/10.1063/1.5067050
View Table of Contents: http://aip.scitation.org/toc/apc/2033/1
Published by the American Institute of Physics

Thermodynamic Simulation of a Hybrid Thermo-Solar Externally Fired Gas Turbine Power Plant Fueled with Biomass

Agustín Ghazarian[1], Daiana De León[1], Pedro Galione[1, b)], Pedro Curto-Risso[1], Alejandro Medina[2, a)], Antonio Calvo[2]

[1]*Departamento de Termodinámica Aplicada, Universidad de la República, Montevideo, Uruguay.*
[2]*Professor. Department of Applied Physics, University of Salamanca, Salamanca, Spain; + 34 677565486.*

[a)]Corresponding author: amd385@usal.es
[b)]pgalione@fing.edu.uy

Abstract. A thermodynamic model for a hybrid thermo-solar externally fired gas turbine power plant fueled with biomass is presented. This technology represents a fully renewable way of obtaining electric power relying mainly in biomass with an extra advantage of decreasing its consumption at good radiative conditions. A concentrated solar power plant is implemented considering the Solugas project situated in Abengoa's Solúcar Platform near Seville. To predict its behavior two models were implemented and compared with experimental data. Typical daily evolution of the output power, biomass mass flow, overall efficiency and biomass conversion efficiency for a typical Uruguayan year is presented. In addition, global results are presented leading to a 1.5% biomass saving increasing the economic efficiency a 0.34% what denotes the solar field and thermal power of receiver seem to be undersized.

INTRODUCTION

Sustainable development of countries relies, among other factors, on the production of energy with reduced greenhouse gases emissions and conserving soil and water. Thus, future energy world supply will be related to a wide variety of energy resources, especially including renewable ones. Besides, energy production in a particular region should be related to its natural energy resources, as for instance solar and biomass. On other hand, gas turbines versatility, dynamic operation and reduced water consumption enable them to operate in a standard open cycle way by using traditional fuels or taking advantage of solar resources or biomass in regions with good insolation or biomass stocks. This is feasible because gas tubines can work both in a closed cycle or externally fired (EFGT) [1].

The combination of solar and biomass energy sources could be interesting due to the resulting increased versatility. Availability of biomass may not be constant throughout the year as well as it is for solar energy. Therefore, this combination, together with some stock managing, could possibly eliminate or diminish the need of thermal storage, and result in a high capacity factor of the power plant.

Biomass typically needs to be transported from its production site to the power plant, and therefore it has an associated cost (both economic and environmental). Thus, the available biomass may not be all "economically" usable. In a recent study [2], the potential for power production using agricultural residues in Uruguay has been assessed, and following work concluded that using only the available agricultural residues, plants of no more than 10 MW are feasible (to be published). By integrating biomass and solar resources into one power plant would allow to have higher power and efficiency.

The aim of this work is to present and validate a thermodynamic model for an EFGT power plant hybridized with a central tower solar receiver. This scheme would provide electric energy in a purely renewable way. Previous works have focused on the hybridization of standard natural gas turbines with a solar subsystem [3] or on the

SolarPACES 2017
AIP Conf. Proc. 2033, 040014-1–040014-9; https://doi.org/10.1063/1.5067050
Published by AIP Publishing. 978-0-7354-1757-1/$30.00

evaluation of the performance of EFGTs with several types of biomasses [4]. But to our knowledge, there are not many, neither experimental nor computational, works on biomass fueled EFGTs hybridized with a central tower solar field.

A modification of the Solugas plant [5] is here explored, by using an external combustion instead of internal, due to the use of solid biomass as a fuel. Except for the combustion part, the studied configuration is the same as that of Solugas plant. Only the Brayton cycle part is studied here, leaving out its integration with a bottoming Rankine cycle. Since the objective of this work is to develop a model capable of simulating the combination of solar tower plants, biomass combustion and Brayton cycles, an optimization of the plant configuration is not performed here, and is left for a future work. Special attention is paid to the modeling of the solar tower power plant, since most of the other models are adopted from previous works. Furthermore, a study of the performance of the plant is carried out, and conclusions regarding possible improvements are included.

MATHEMATICAL MODELING AND CASE DEFINITION

The cycle starts when air at ambient conditions (pressure P1 and temperature T1) passes through Nc non adiabatic compressors equipped with (Nc-1) intercoolers to finally reach pressure P2 and temperature T2. The intercoolers are situated between each pair of compressors to decrease the air exit temperature to T1 before entering the next compressor. After this process the air is pre-heated in a solar tower before reaching the entrance of a high temperature heat exchanger (HTHE). In the HTHE the air is heated by combustion gases coming from a combustion chamber to temperature T3, which must be settled taking into account constructive and metallurgical limits. In order to reach this temperature, the biomass mass flow entering the combustion chamber is calculated. After heated, the air is expanded through a turbine to pressure P4 and temperature T4. The expanded air enters the combustion chamber, where it is burned along with the biomass, and after exchanging power in the HTHE it is released to the ambient. A scheme of the plant is presented in Fig. 1.

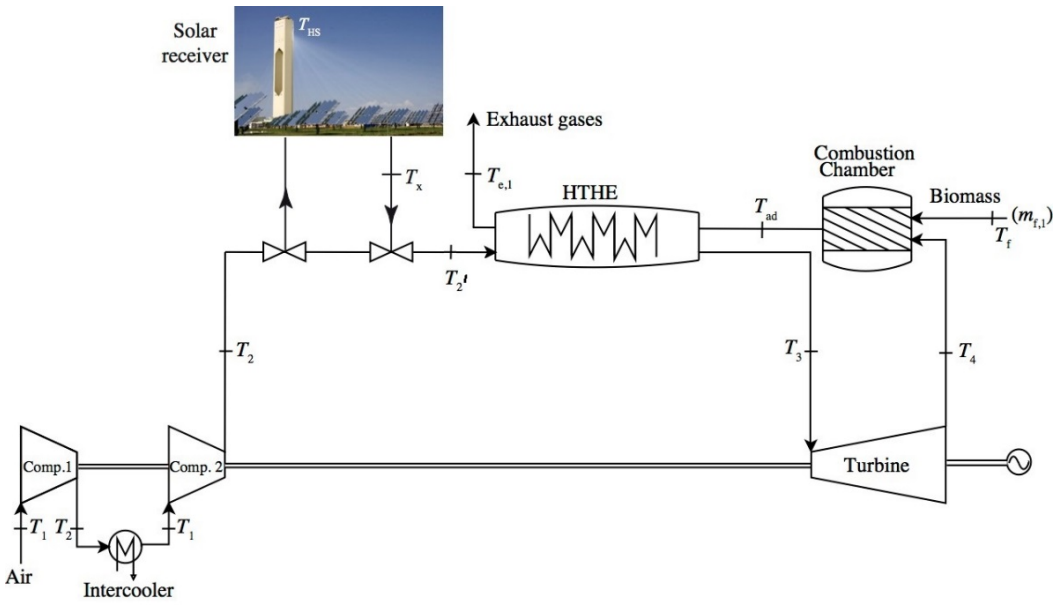

FIGURE 1. Plant scheme.

Plant Model

As the actual receiver placed in Solugas allows a 5.6 kg/s air mass flow, a bypass was implemented. The air exiting the compressor (at temperature T_2) is divided before the receiver and mixed afterwards before the HTHE entrance. As shown in figure 1, the air exiting the receiver reaches temperature T_x while the temperature at the HTHE entrance is $T_{2'}$. The plant model is the one presented in [6].

The combustion chamber and heat exchanger models consist in solving the combustion, energy balances and heat transfer problems. Compressors and turbine are modeled as two non-isentropic processes by considering the ideal isentropic process and taking into account the isentropic efficiencies (please refer to [6] for further details).

The amount of biomass needed is calculated by solving the heat needed by the air to reach T_3 (fixed) in the HTHE, and with this the needed adiabatic temperature T_{ad} that should be reached at the exit of the combustion chamber. The way of controlling this temperature is by varying the combustion equivalence ratio.

In this work, a HTHE with efficiency of around 0.70 is adopted. This value could be improved and efficiencies as high as 0.9 could be reached using ceramic heat exchangers [6].

Solar Power Tower Model

The solar receiver considered in the model is the one placed in the SOLUGAS tower (Fig. 2) developed by ABENGOA in 2009, situated in Spain. The central tower (77m height) is pointed by a maximum number of 69 heliostats, each one of 121.3m^2. The receiver consists of 10 panels, each one formed by 17 absorber tubes, with an inlet diameter of 19.6mm, an outer diameter of 22.4mm and a total length of 5m.

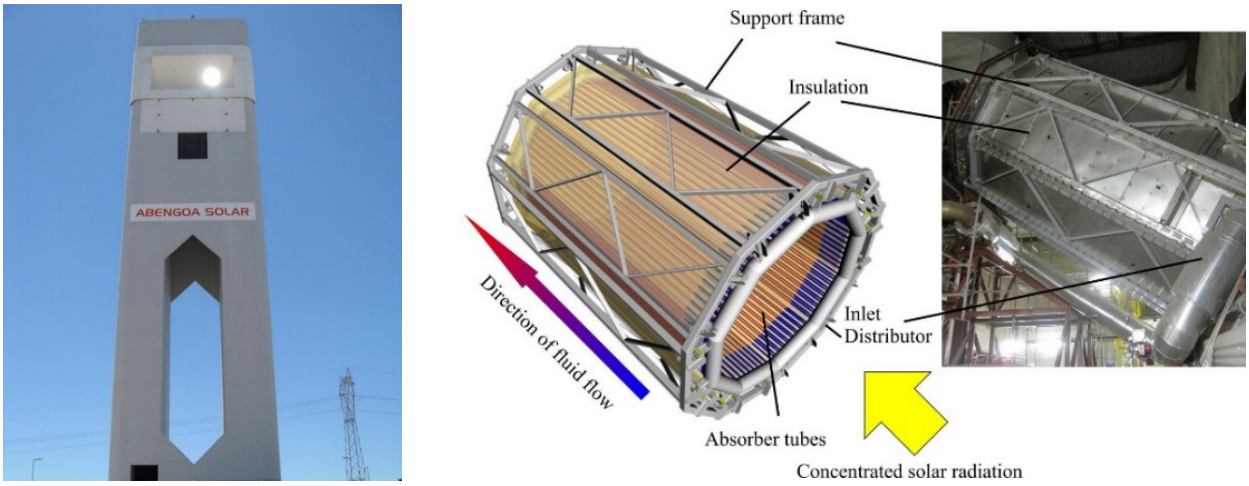

(a) Tower (b) Receiver

FIGURE 2. Pictures of the central tower (a) and the receiver (b) of the Solugas project. Reprinted from [5] with permission from Elsevier.

Two models were implemented for solving thermal performance. The main difference between them is the way in which radiation heat exchange inside the cavity is modeled.

Model 1

This model is presented in [7] and consists on the following balance.

$$Q_{air} = \eta_{sol} G A_{col} - \varepsilon_{eff} \sigma A_{rec} \left({T_{rec}}^4 - {T_{amb}}^4 \right) - U_L A_{rec} (T_{rec} - T_{amb}) \quad (1)$$

Where Q_{air} is the heat gained by the air in the receiver, η_{sol} the fraction of the incident radiation that reaches the receiver, G the direct normal irradiance, A_{col} the aperture area of the collector, A_{rec} the absorber area of the receivers, ε_{eff} the effective emissivity, σ the Stefan-Boltzmann constant, T_{amb} the ambient temperature (K), T_{rec} the temperature of the surface of the receiver and U_L the convective losses of the solar receiver. η_{sol} was estimated using experimental data [8] shown in Table 1.

TABLE 1. Reference data obtained from [8].

DNI	Aligned heliostats	Heliostat area	Solar Input Power into receiver
910.4 (W/m^2)	67	121.3m^2	3.72MW

The effective emissivity of the receiver ε_{eff} was calculated by considering an emissivity value of 0.9 [9] for the tubes in a cylindrical cavity and affecting it by the view factor between the tubes and cavity apertures, as proposed in [10]. As there is no experimental data regarding the convection coefficient U_L, the following approach was considered for its determination. Solar input power, thermal output power and T_{rec} obtained from [5] were used as input data in Eq. (1), and a least squares method was applied in order to find the coefficient which better fits this experimental information. The final values obtained where $U_L A_{rec}$= 740$\frac{W}{K}$, ε_{eff}= 0.11, η_{sol} = 0.50 and the error committed with the least squares method varies between 2% and 11%.

Model 2

The second model considers a cylindrical cavity formed by 3 surfaces which receives energy at solar spectrum and emits in infrared frequencies. Surface 1 represents the cavity aperture (considered as a black body at ambient temperature), surface 2 the absorber tubes area and surface 3 the back wall (considered as completely back-insulated without convection losses). Convection losses are taken into account only in surface 2. A radiosity method [11] is implemented to solve the cavity, at both, the solar and infrared spectrum. The heat gained by the surfaces at the solar spectrum (Q_2 and Q_3) is then released at infrared spectrum as shown below.

At solar spectrum:

$$J_{1s} = \eta_s \sigma A_{col} \tag{2}$$

$$A_2 J_{2s} = \rho_2 (A_1 J_{1s} F_{12} + A_2 J_{2s} F_{22} + A_3 J_{3s} F_{32}) \tag{3}$$

$$A_3 J_{3s} = \rho_3 (A_1 J_{1s} F_{13} + A_3 J_{2s} F_{32}) \tag{4}$$

The heat gained by the surface 2 and 3 can be expressed in the following way.

$$Q_2 = (J_{3s} - J_{2s}) F_{32} A_3 + (J_{1s} - J_{2s}) F_{12} A_1 \tag{5}$$

$$Q_3 = (J_{1s} - J_{3s}) F_{13} A_1 + (J_{2s} - J_{3s}) F_{32} A_3 \tag{6}$$

At infrared spectrum:

$$Q_3 = (J_3 - J_2) F_{32} A_3 + \left(J_3 - \sigma {T_{amb}}^4\right) F_{13} A_1 \tag{7}$$

$$(J_3 - J_2) F_{32} A_3 + \left(\sigma {T_{amb}}^4 - J_2\right) F_{12} A_1 = \left(J_2 - \sigma {T_{rec}}^4\right) \frac{\varepsilon_2 A_2}{1-\varepsilon_2} \tag{8}$$

$$\left(J_2 - \sigma {T_{rec}}^4\right) \frac{\varepsilon_2 A_2}{1-\varepsilon_2} + Q_2 = Q_{air} + h(T_{rec} - T_{amb}) A_2 \tag{9}$$

Where J_{is} and J_i represents the i surface radiosity at solar and infrared spectrum respectively, η_s the optical efficiency of the field (0.5 as in Model 1), ε_i and ρ_i the i surface emissivity and reflectivity, T_{rec} the temperature of the surface of the receiver, T_{amb} the ambient temperature, h the convective losses coefficient (calculated with a least squares method as in Model 1), A_i the i surface area and F_{ij} the i and j view factor. Q_{air} is the heat gained by the air in the solar receiver. hA_2 product resulted in 659 W/K, which is somewhat lower than the value of *UA* obtained with model 1.

T_{rec}, Q_{air} and T_x are determined using either Model 1 or 2, together with an $\varepsilon - NTU$ method for the air inside tubes. Values of T_x predicted by both models are plotted against experimental data [8] in Figure 3, where it can be observed that model 2 provides a more accurate description while model 1 tends to overestimate T_x.

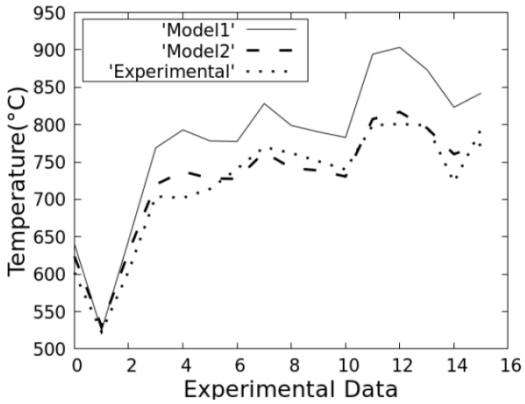

FIGURE 3. Receiver outlet temperature (T_x) predictions against experimental data [8] at different operating points.

Case Study

One year simulation in Montevideo, Uruguay, was run using biomass with the following composition C = 49.3%,
H = 6%, O = 44.4%, N < 0.01%, Ash = 0.3% with a low heating value (LHV) of 18681 kJ/kg, considering the irradiation and ambient temperature data obtained from [12]. Annual DNI in Montevideo is 1760 $\frac{kWh}{m^2}$ and temperature and DNI evolution in typical summer and winter days are presented in Figure 4.

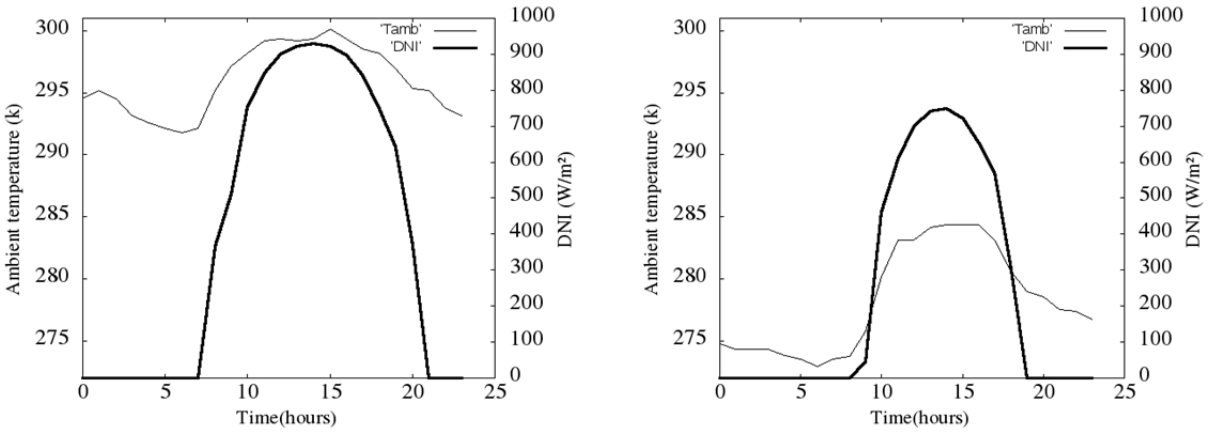

(a) Summer. (b) Winter.

FIGURE 4. Ambient temperature and DNI evolution for typical summer and winter days.

Power output, biomass mass flow, total and economic efficiency curves for these typical days are presented in the results section. Total efficiency is calculated as the obtained output power divided over the power entering the plant Eq. (10), while the economic efficiency is the ratio between the net power produced and the input energy associated to the biomass Eq. (11).

$$\eta_{total} = \frac{Net\ Output\ Power}{\dot{Q}_s + \dot{m}_b h_b + \dot{m}_a h_a} \tag{10}$$

$$\eta_{econ} = \frac{Net\ Output\ Power}{\dot{m}_b LHV} \tag{11}$$

Where $\dot{Q}s$ stands for the solar input power, $\dot{m}_b$ and h_b the biomass mass flow and enthalpy respectively. Finally, $\dot{m}_a$ and h_a represent air mass flow and enthalpy.

Mercury 50 Gas turbine was considered in the model. The main turbines parameters are shown in Table 2 while the pressure loss in the installation is taken as an input parameter. The compressor and turbine isentropic efficiencies were obtained considering data presented in [5] where ambient temperature, the compressor discharge gauge pressure, the turbine inlet temperature and the compressor discharge temperature where specified. For the determination of both efficiencies a 16.7 $\frac{kg}{s}$ was employed.

TABLE 2. Turbine parameters.

Item	Quantity
Power ISO conditions	4600kW
Pressure ratio	10
Mass flow	16.7(kg/s)
Compressor efficiency	0.843
Turbine efficiency	0.822

RESULTS

In Fig. 5 it can be noted that the net output power increases in winter. This can be explained since the power obtained from the turbine remains constant as the inlet temperature is a fixed parameter, while the power required by the compressor decreases as the ambient temperature is lower, leading to an increase in air density.

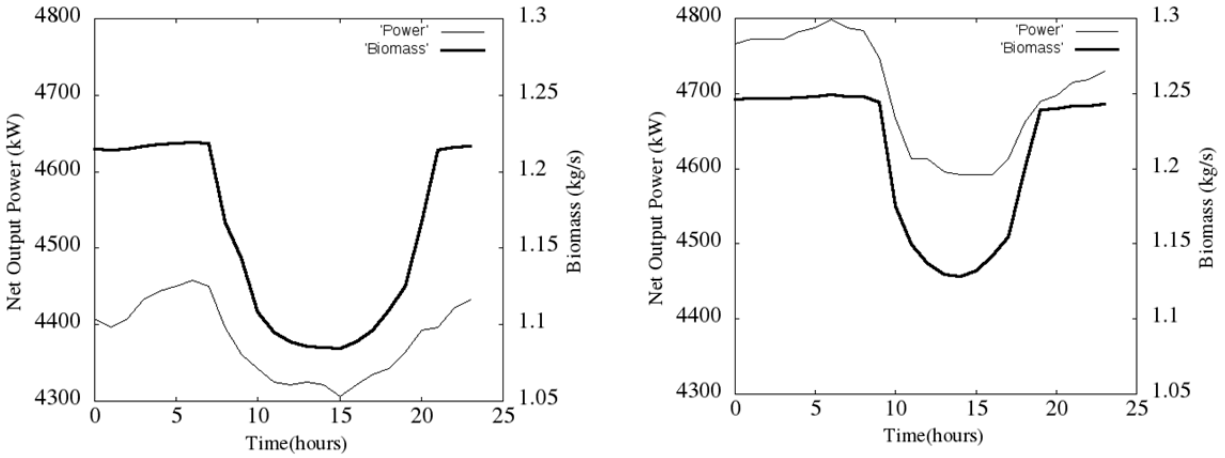

(a) Summer. (b) Winter.

FIGURE 5. Net output power and biomass mass flow for typical days.

Due to lower ambient temperature and solar irradiance, an increase in biomass consumption during winter is expected. This effect can be also observed in Fig. 5.

The total plant efficiency is below 0.20 which is lower than other hybrids plants presented, for example in [5] a total efficiency of 0.27 is predicted. This difference can be explained since the model considers an externally fired gas turbine, this leads to higher gases temperature which means higher spillage in the exhaust gases. Economic efficiency reaches values of around 0.215.

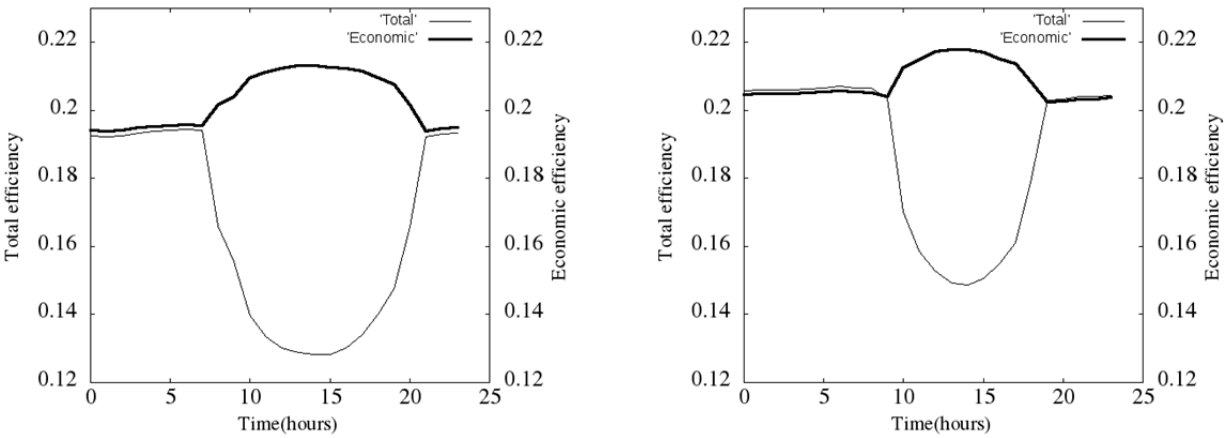

FIGURE 6. Evolution of the overall plant efficiency and the biomass conversion efficiency as functions of time during typical summer and winter days.

In Fig. 7 typical summer and winter daily temperature evolution is shown. It can be noted that T_4 remains constant (as expected by setting T_3), while small variations of ambient temperature can be appreciated. The main difference lies in the collector outlet temperature, which reaches temperatures of about 1100 K in summer and 800 K in winter.

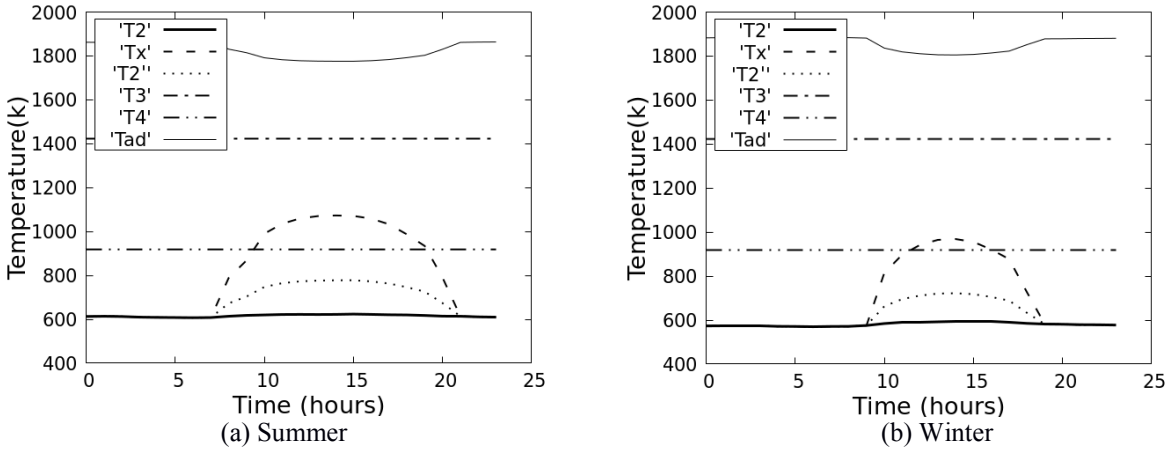

FIGURE 7. Evolution of main temperatures in the thermodynamic cycle for typical summer (a) and winter (b) days.

In order to obtain global results, a comparison between the hybrid and non-hybrid plant for a year simulation is performed. It must be noted that the power obtained is the same since it only relies on the ambient temperature, compressor isentropic efficiency, turbine isentropic efficiency and the fixed temperature T3.

The total energy obtained is 141.78 TJ with a predicted biomass consumption of 3.8×10^7 kg for the hybrid plant, what leads to a 20% economic efficiency. On the other hand, without considering the solar tower and with the same HTHE, the biomass mass predicted ascends to 3.86×10^7 kg, leading to an economic efficiency of 19.66%.

CONCLUSIONS

A thermodynamic model for a hybrid thermo-solar externally fired gas turbine power plant fueled with biomass was successfully developed. Two models for the radiation losses in the tower cavity were implemented and tested.

Power output and total and economic efficiencies for a plant situated in Uruguay were obtained from a year simulation.

Most important results were:

- The power obtained from the plant varies between 4800(kW) and 4200 (kW), reaching the maximum during winter due to a decrease in the compressors power consumption.
- As expected, the biomass required during winter results higher than in summer, due to both the lower irradiation and lower ambient temperature.
- A 2% rise can be observed in the instant economic efficiency at good radiation conditions.
- Due to the low biomass savings it can be noted that the solar field and solar receiver seem to be undersized. This can also be appreciated considering that at the best radiation conditions the solar energy represents only a 25% of the total energy needed.
- In Solugas plant, a maximum temperature of 650 ºC is allowed at the combustion chamber entrance. In this work, since the combustion is external, this restriction could be removed. However, some limitations to this temperature could exist due to technological issues in the HTHE.
- An increase in the plant efficiency could be reached if a bottoming cycle is considered, using the available energy of the combustion gases exiting the HTHE or the air exiting the turbine.

FUTURE RESEARCH

- The design of an appropriate solar field and solar receiver, leading to greater temperatures at the tower outlet and an increment in the mass flow allowed at this component should be considered.
- A bottoming cycle implementation should be included in order to obtain reasonable efficiencies.
- Different plant configurations, as well as dimensioning of the solar plant and HTHE, should be evaluated. Optimization analyses leading to highest energy efficiencies and/or lowest costs should be performed.

ACKNOWLEDGMENTS

A.M. and A.C.H. acknowledge financial support from University of Salamanca. A.G., D.D.L., P.G. and P.C. acknowledge support from ANII, Uruguay, through project FSE_1_2015_1_110011.

REFERENCES

1. M. Kautz and U. Hansen. The externally fired gas turbine (EFGT-cycle) for decentralized use of biomass, Appl. Ener., 84, 795-805 (2007).
2. G. Pena, A. Durante, P. Curto, E. Franco, A.C. Pina, A. Amaya, N. Tancredi. “Characterization of residual biomass from agricultural and agroindustrial activities,” in Proceedings of the 24th ABCM International Congress of Mechanical Engineering, Curitiba, Brazil, 2017.
3. M. Jamel, A. Abd Rahman and A. Shamsuddin. Advances in the integration of solar thermal energy with conventional and non-conventional power plants, Renew. Sust. Ener Rev., 20, 71-81 (2013).
4. K. Al-Attab and Z. Zainal. Externally fired gas turbine technology, Appl. Ener., 138, 474-487 (2015).
5. R. Korzynietz, J.A. Brioso, A. del Río, M. Quero, M. Gallas, R. Uhlig, M. Ebert, R. Buck, D. Teraji. Solugas – Comprehensive analysis of the solar hybrid Brayton plant, Sol. Ener., 135, 578-589 (2016).
6. A. Durante; G. Pena-Vergara; P.L. Curto-Risso; A. Medina; A. Calvo Hernández. Thermodynamic simulation of a multi-step externally fired gas turbine powered by biomass, Ener. Conv. Manage., 140 (15) 182-191 (2017).
7. M.J. Santos, R.P. Merchán, A. Medina, A. Calvo Hernández. Seasonal thermodynamic prediction of the performance of a hybrid solar gas-turbine power plant,. Ener. Conv. Manage., 115, 89-102 (2016).
8. M. Ebert, D.Benitez, M. Röger, R. Korzynietz, J.A. Brioso. Efficiency determination of tubular solar receivers in central receiver systems. Sol. Ener., 139 (1), 179-189 (2016).
9. R. Uhlig (private communication).

10. K. Lovergrove, “Fundamental principles of concentrating solar power (CSP) systems,” in *Concentrating solar power technology*, edited by K. Lovergrove and W. Strein (Woodhead Publishing, 2012), pp. 16–66.
11. T. Bergman, A. Lavine, F.Incropera, D. Dewitt, “Radiation Exchange Between Surfaces” in Fundamentals of heat and mass transfer, Wiley, 2012.
12. Laboratorio de Energía Solar. www.unorte.edu.uy/uy